

Thermal Resistance of Thermal Barriers in polycrystalline Diamond

J. Hartmann, M. Reichling, and E. Matthias

*Freie Universität Berlin, Fachbereich Physik, Arnimalle 14, 14195 Berlin, Germany
e-mail: reichling@matth1.physik.fu-berlin.de, fax: +49-30-838-6059*

Abstract. Micrometer resolved photothermal measurements on chemical vapour deposited (CVD) diamond are presented. It is shown that the thermal conductivity inside the grains is as high as that of natural IIa diamond. Using two different approaches we measure the thermal resistance of thermal barriers like grain boundaries or microcracks and obtain values of the order of 10^{-9} m²K/W. A simple model is presented, relating the overall thermal conductivity for one-dimensional heat flow to the thermal resistance at barriers and the average size of the grains. Good agreement between predictions and literature data is found.

1. INTRODUCTION

As diamond has the highest room temperature thermal conductivity of all known materials and also high electrical resistivity, it is a promising material for thermal management applications in electronic devices.¹ Deposition technologies now offer the possibility to grow synthetic diamond films with physical properties close to those of natural diamond.² However, synthetic diamond grown by chemical vapour deposition (CVD) is polycrystalline and composed of single grains that are separated from each other by boundaries² and microcracks resulting from sample preparation like polishing.³ These grain boundaries and microcracks act as effective thermal barriers and yield a lower in-plane thermal conductivity. Several authors investigated the thermal properties of diamond in different modifications using the photothermal mirage^{4,5} and transient thermal grating-techniques⁶. All these measurements yielded results averaged over at least several grains and did not provide a resolution required for the investigation of individual grains and thermal boundaries.

In this work we use a high-resolution photothermal microscope⁷ to determine local thermal properties with micrometer resolution. Our goal is to investigate thermal barriers in CVD-diamond layers and to relate their thermal resistance to the overall thermal conductivity of the sample.

2. EXPERIMENTAL

We use a tightly focused, modulated Ar⁺-laser beam to generate thermal waves, and detect the resulting surface temperature via the modulated reflectance of a HeNe-laser beam. The experimental setup is incorporated in a commercial microscope allowing laser spot diameters on the sample surface of approximately 1µm, necessary for measurements with high lateral resolution. The large thermal conductivity of CVD-diamond samples requires high modulation frequencies of 5-12 MHz to obtain a reasonably short thermal length. Details of the apparatus are discussed elsewhere.⁷ The local nature of such measurements allows the use of an analytical, three-dimensional model for data evaluation including only one thermal barrier under investigation and half-infinite adjacent grains.^{8,9}

Two different procedures are used to obtain quantitative information about the height of the thermal barriers. In **mode 1**: we measure thermal profiles by varying the distance between

pump and probe beam, keeping the thermal barrier and the probe laser beam fixed at a certain distance while scanning the pump laser beam. **mode 2:** We keep the distance between pump and probe beam fixed and move the thermal barrier with respect to both laser spots.¹⁰ In both cases we record the phase of the photothermal signal as a function of the scanned distance. The sample under investigation was a free-standing CVD diamond plate of $10 \times 10 \times 0.6 \text{ mm}^3$ covered with a 20 nm gold layer to obtain a homogeneous surface absorption and thermo-reflectance signal.

3. RESULTS

To obtain an overview of the region of interest, we performed two-dimensional raster scans using scanning mode 2 at 1, 3 and 5 MHz modulation frequency, respectively. The photothermal amplitude maps of these scans together with a CCD camera image are shown in Fig. 1. The photothermal amplitude exhibits a clear grain boundary structure that is only barely visible in the microscopy image.

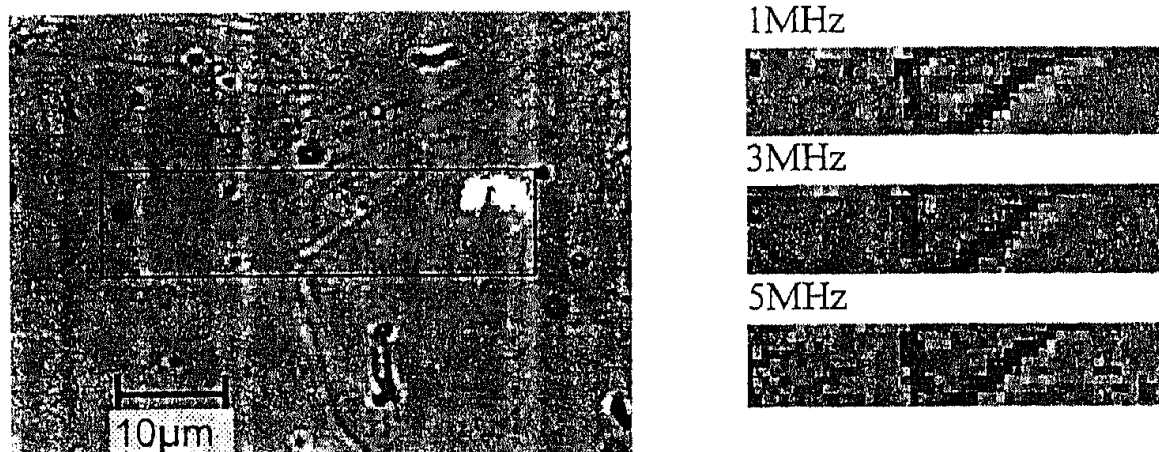


Figure 1: Microscopy image of the sample surface (left) also showing the laser spots. The photothermally scanned area of $10 \times 50 \mu\text{m}^2$ is shown as a rectangle. Photothermal amplitude maps at 1, 3 and 5 MHz modulation frequency are shown on the right side.

For quantitative measurements we performed line scans in scanning mode 1 and 2. Figure 2 shows a phase profile obtained in scanning mode 1 with the pump beam crossing a thermal barrier at $6 \mu\text{m}$ distance from the probe beam. When the pump beam is far away from the thermal barrier, the slope of the phase curve is constant. As soon as the pump beam approaches the thermal barrier, thermal wave interference occurs yielding a smaller slope. Immediately after crossing the thermal barrier the phase drops steeply while a further increase

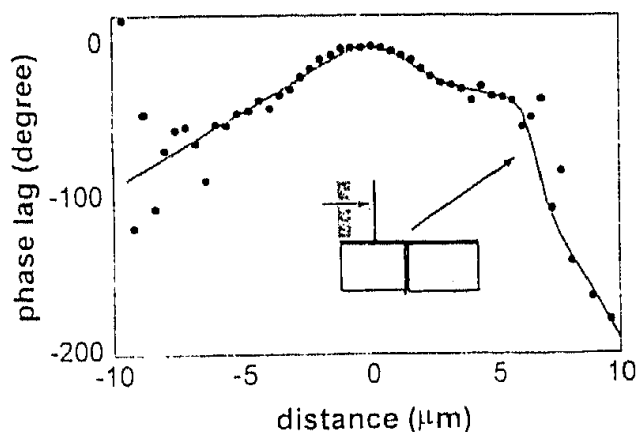


Figure 2: Photothermal phase profile at 12 MHz for a scan across a thermal barrier (dashed line). The probe beam was fixed at the origin while the pump beam was scanned along a straight line crossing probe beam and thermal barrier (mode 1). The solid line is a fit of the thermal model to the experimental data.

in distance again yields a straight line. The best fit of the thermal model to the data shown by the solid line is obtained for a thermal conductivity $\kappa_1=2300\text{W/mK}$ in the grain on the left side of the boundary, $\kappa_2=300\text{W/mK}$ for the grain on the right side and $R_{th}=8.5\times 10^{-9}\text{m}^2\text{K/W}$ for the thermal resistance at the interface.

A measurement performed in mode 2 at a different thermal barrier on the same sample yields a phase development as shown in Fig. 3. As long as both beams are distant more than the thermal length from the thermal barrier, we observe a constant phase. Approaching the grain boundary, the phase first rises to drop sharply when the beams are separated by the thermal barrier. Fitting the data with the thermal model yields $\kappa_1=2300\text{W/mK}$ in the grain on the left side of the boundary, $\kappa_2=1200\text{W/mK}$ for the grain on the right side and $R_{th}=2\times 10^{-9}\text{m}^2\text{K/W}$ for the thermal resistance at the interface. As the second method is more sensitive to lateral heat flow, we assume the lower value for the thermal resistance as the more reliable.

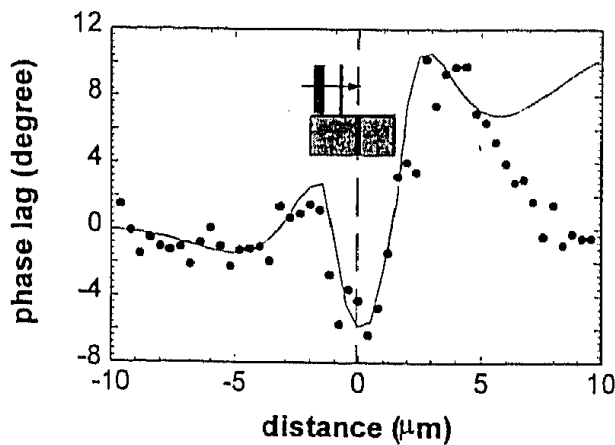


Figure 3: Photothermal scan at 12MHz across a thermal barrier at $x=0$ (indicated by the dashed line). Pump and probe beam are separated by $3\mu\text{m}$ (mode 2). The solid line is a fit of the thermal model of the experimental data.

Using the obtained values for the thermal conductivity within the grains and the thermal resistance together with a simple model for the grain structure in the sample we are able to estimate the total lateral thermal resistance from the contribution of all thermal barriers. Assuming a sample with length A having cubic grains with an average length a , the total quantity of grain boundaries within the sample is $(A/a - 1)$. The thermal resistance R_{1dim} for one-dimensional heat flow across the sample is then the sum of the thermal resistance of the bulk material A/κ and the additional resistance R_{th} from the grain boundaries, yielding

$$R_{1dim} = A/\kappa + R_{th}(A/a - 1).$$

Using this formula, an overall thermal conductivity for one-dimensional heat flow κ_{1dim} can be estimate as

$$\kappa_{1dim} = A/R_{1dim} = A/(A/\kappa + R_{th}(A/a - 1)),$$

reducing to

$$\kappa_{1dim} = 1/(1/\kappa + R_{th}/a)$$

for $A \gg a$. This simple relation offers a practically useful way for calculating the thermal conductivity of a polycrystalline sample resulting from one-dimensional heat flow experiments only by the knowledge of the average grain size. Taking the average grain size for our sample ($a=15\mu\text{m}$) this procedure yields a one-dimensional overall conductivity $\kappa_{1dim}=1663\text{W/mK}$, well in accordance with measurements of comparable samples presented in literature.^{2,11}

The model can be used to evaluate overall thermal conductivities for CVD-diamond data by Graebner et al.¹¹, where grain size and overall thermal conductivity of a series of CVD-diamond samples were presented. Using our one-dimensional model, a conductivity of

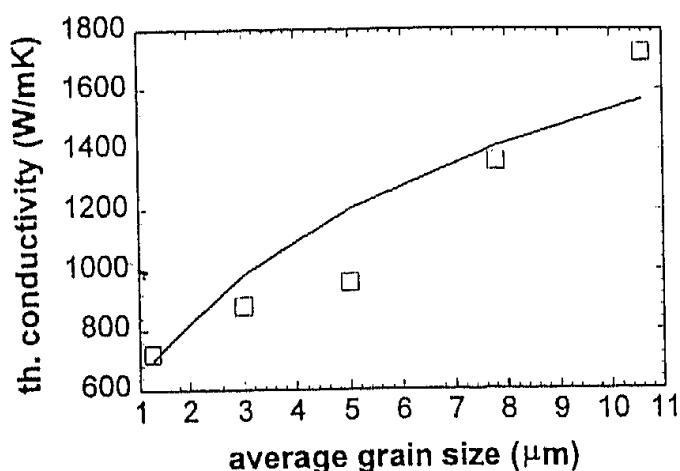


Figure 4: Comparison of the dependence of the overall thermal conductivity of CVD diamond on the average grain size predicted using results from a local thermal analysis (solid line) with experimental data of Graebner et al.¹¹ (squares).

2300W/mK, a thermal resistance of $2 \times 10^{-9} \text{ m}^2 \text{ K/W}$ and the grain sizes given in Ref. 11 we obtain a thickness dependence of the overall one-dimensional conductivity as shown in Fig. 4. Considering the simplicity of the model and that we calculated conductivities a priori without any fit to the data from Ref. 10, there is a surprisingly good agreement between measured data and our predictions.

4. ACKNOWLEDGMENTS

This work was supported by the Deutsche Forschungsgemeinschaft, Sfb337 and the DAITM project of the Brite Euram Program. Sample preparation by GEC Marconi, Towcester is gratefully acknowledged.

5. REFERENCES

1. B. Fliegl, R. Kuhnert, H. Schwarzbauer, F. Koch, *Diamond and Related Materials* 3, 658 (1994)
2. J.E. Graebner, S. Jin, J.A. Herb, C.F. Gardinier, *J. Appl. Phys.* 76(3), 1552 (1994)
3. K.M. McNamara Rutledge, B.E. Scruggs, K.K. Gleason, *J. Appl. Phys.* 77(4), 1459 (1995)
4. T.R. Anthony, W.F. Bannholzer, J.F. Fleischer, L. Wie, P.K. Kuo, R.L. Thomas, R.W. Pryor, *Phys. Rev.* B42(2), 1104 (1990)
5. D. Fournier, K. Plamann, *Diamond and Related Materials* 4, 809 (1995)
6. O.W. Käding, H. Skurk, A.A. Maznev, E. Matthias, *Appl. Phys.* A61, 253 (1995)
7. J. Hartmann, M. Reichling, E. Matthias, *J. Appl. Phys.*, submitted
8. A.M. Mansanares, T. Velinov, Z. Bozoki, D. Fournier, A.C. Boccara, *J. Appl. Phys.* 75(7), 3344 (1994)
9. F. Lepoutre, D. Balageas, Ph. Forge. S.Hirschi, J.L. Joulaud, D. Rochais, F.C. Chen, *J. Appl. Phys.* 78(4), 2208 (1995)
10. G. Meyer-Berg, R. Osiander, P. Korpiun, P. Kakoschke, *Springer Series in optical Science, Vol. 69, Photoacoustic and Photothermal Phenomena III*, Ed.: D. Bicanic, Springer Verlag, Berlin Heidelberg (1992), p. 711
11. J.E. Graebner, S. Jin, G.W. Kammlott, J.A. Herb, C.F. Cardinier, *Appl. Phys. Lett.* 60(13), 1576 (1992)